



Numerical modeling of NOx by using micro combustor

Maryam Sabeti¹, Javad Abolfazli Esfahani^{1,*}

¹ Department of Mechanical Engineering, Ferdowsi university of Mashhad, Mashhad, Khorasan Razavi, Iran, +98

*Corresponding Author: E-mail: Jaesfahani@gmail.com, Telephone Number: +989358185400, Fax. Number: +985118829441

Abstract

The present study focused on numerical modelling on flame temperature and pollutant emissions of H₂-air mixture combustion in a series of chambers with same shape and various diameters under adiabatic wall condition. The simulation results indicate that increasing the flame temperature and the combustion efficiency by increasing diameter, decreasing the NO_x emission by depleting chamber size and the zero emission of the prompt NO_x emission by using hydrogen as fuel in micro combustors. Also the best chamber size of reducing NO_x emission and high efficiency was achieved at chamber diameter about 5 to 70 mm.

Keywords: Micro combustion; Hydrogen; Premixed mixture; Numerical model; NO_x emission

1. Introduction

There has been increasing in mobile miniature and micro devices, such as micro-robots, actuator and personal electrical products, the needs for a micro power source are increasing to activate these systems [1]. The interaction between MEMS (Micro Electro Mechanical Systems) technology and knowledge of conventional energy generating principal has recently evolved into an area known as power MEMS. Thus, during the last decade, many feasibility studies have focused on the development of new portable power generation system that use a fuel such as hydrocarbon or hydrogen as an energy source [2]. Indeed, these systems were mainly agitated by the fact that hydrogen and most hydrocarbon fuels have

much higher energy density [3]. The miniature and micro scale combustors are the key components of the miniaturized power and propulsion systems, it's well known that at smaller scales, heat losses play an important role in flame stability and its temperature due to the increased ratio of surface area to volume in a small-scale combustor [4]. Thus, various researchers have attempted to know about the structure of flame, its temperature and stabilization inside a small-scale combustor. Despite extensive attempt to know of combustion mechanism in micro-scaled combustors, many behaviors of combustion isn't understood as well as these actions in large-scaled combustors to design or optimization [5]. Due to many difficulties occur when



measuring the physical quantities of interest at small scales, numerical simulation of small-scale combustors are especially important to determine the combustion features that are required for combustor designs [6 - 8].

Recently, attention has also been focused on the pollutant emission characteristics of combustion. Nitrogen oxides (NO_x=NO+NO₂) are major pollutants, since they are very harmful, and cause secondary air pollution problems, such as ozone depletion and photochemical smog.

In this paper, computational fluid dynamics based numerical simulation have been performed to study the combustion of H₂-air mixture in a series of chambers with same shape aspect ratio but various dimensions have been undertaken by solving the 2D governing equations. Indeed, the effect of chamber size from large scale to micro-scale pollution emission such as NO_x in the combustion chamber is investigated by numerical simulations.

2. NUMERICAL MODEL

2.1. Geometry and fluid flow model

Figure.1 shows the geometry of the cylindrical micro-combustor used in this paper. The inlet diameter (D) of the chamber is changed from the micro size to the macro size but at this model the ratio of the inlet diameter to chamber diameter is fixed at 0.5 and the ratio of chamber length to inlet diameter is maintained at 15.50 for all sizes. Stoichiometric H₂-air mixture is injected into the cylindrical combustor from the inlet. The case is simplified to a 2D axi-

symmetric problem. Axi-symmetric boundary conditions are applied along the central axis of the combustion chamber. In addition, the following assumption are made: (1) no gas radiation [9,10]; no work done by pressure and viscous forces is applied; (2) no slip boundary condition on the wall is considered (3) steady-state and laminar regimes are applied; (4) The inlet temperature of fuel mixture is considered to be uniform at 300k ; (5) A fixed uniform velocity is specified at the inlet; (6) At the exit pressure outlet boundary condition is specified with a fixed pressure of 1.013*10⁵ pa; (7) An adiabatic boundary condition at all wall of the chamber is applied. With this assumption, the Navier-stokes equation is solved for fluid domain and the governing equations are discretized using the finite-volume method and solved by computational fluid Dynamics (CFD) [3]. The governing equations of continuity, momentum, species and energy in the gas phase for the cylindrical micro-combustor can be written as follows [11, 12]. X depicts the axial distance and r represents the radial distance or distance from the centre line of the cylindrical chamber, respectively.

Continuity:

$$\frac{\partial \rho}{\partial t} + \frac{\partial(\rho u)}{\partial x} + \frac{\partial(\rho v)}{\partial r} + \frac{\rho v}{r} = S_m \quad (1)$$

X Momentum:

$$\begin{aligned} & \frac{\partial(\rho u)}{\partial t} + \frac{1}{r} \frac{\partial(\rho u r)}{\partial x} + \frac{1}{r} \frac{\partial(\rho u v r)}{\partial r} = \\ & - \frac{\partial p}{\partial x} + \frac{1}{r} \frac{\partial}{\partial x} \left[r \mu \left(2 \frac{\partial u}{\partial x} - \frac{2}{3} (\nabla \cdot \vec{v}) \right) \right] + \frac{1}{r} \frac{\partial}{\partial r} \left(r \mu \frac{\partial u}{\partial r} \right) \\ & + \frac{1}{r} \frac{\partial}{\partial r} \left(r \mu \frac{\partial v}{\partial x} \right) + F_x \end{aligned} \quad (2)$$

R momentum:



$$\begin{aligned} & \frac{\partial(\rho v)}{\partial t} + \frac{1}{r} \frac{\partial(\rho u v r)}{\partial x} + \frac{1}{r} \frac{\partial(\rho v v r)}{\partial r} = \\ & -\frac{\partial p}{\partial r} + \frac{1}{r} \frac{\partial}{\partial x} \left[r \mu \left(\frac{\partial v}{\partial x} + \frac{\partial u}{\partial r} \right) \right] + \frac{1}{r} \frac{\partial}{\partial r} \left[r \mu \left(2 \frac{\partial v}{\partial r} - \frac{2}{3} (\nabla \cdot \vec{v}) \right) \right] \\ & - 2 \mu \frac{v}{r^2} + \frac{2}{3} \frac{\mu}{r} (\nabla \cdot \vec{v}) + \rho \frac{v^2}{r} + F_r \end{aligned} \quad (3)$$

Energy:

$$\begin{aligned} & \frac{\partial}{\partial x} (\rho u h) + \frac{1}{r} \frac{\partial}{\partial r} (\rho v h r) = \\ & \frac{\partial}{\partial x} \left(k \frac{\partial T}{\partial x} \right) + \frac{1}{r} \frac{\partial}{\partial r} \left(k \frac{\partial T}{\partial r} r \right) - \frac{1}{r} \frac{\partial}{\partial r} \left(r \rho \sum_{i=1}^N Y_i h_i v_i \right) \\ & - \frac{\partial}{\partial x} \left(\rho \sum_{i=1}^N Y_i h_i v_i \right) + q \end{aligned} \quad (4)$$

Species conservation:

$$\begin{aligned} & \frac{\partial(\rho u Y_i)}{\partial x} + \frac{1}{r} \frac{\partial(\rho v r Y_i)}{\partial r} + \\ & \frac{\partial}{\partial x} \left[D_i \frac{\partial(\rho Y_i)}{\partial x} \right] + \frac{1}{r} \frac{\partial}{\partial r} \left[D_i r \frac{\partial(\rho Y_i)}{\partial r} \right] + \omega_i \end{aligned} \quad (5)$$

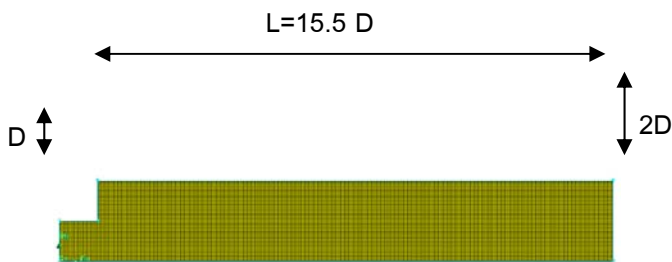


Fig1. Cylindrical-type combustor for micro combustion modeling

The CFD simulation convergence is judged upon the residuals of all governing equations. The results reported in this study are achieved when the residual are smaller than 10^{-6} . The gas density is calculated using the ideal gas law. The gas viscosity, specific heat and thermal conductivity are calculated as a mass fraction-weighted average of all species. The third bodies efficient for all molecular reactions are 2.5 for H_2 , 16 for H_2O and 1.0 for all the rest of species.

The mesh grid size of model was finalized to be $5 \mu m$ for the CFD simulations. Higher and

smaller grid sizes were tested but no obvious advantage was found. All the physical and boundary conditions summarized in this section are applied to all cases in this research. Other conditions such as different inlet velocity may vary from case to case for the purpose of comparison and will be stated in the respective section.

2.2 NOx formation

It is known that during combustion of hydrocarbon fuels, the NOx formation rate can exceed that produced from direct oxidation of nitrogen molecules. Hydrogen is considered an ideal alternative to conventional hydrocarbon fuels, because hydrogen can be produced from any kind of energy source and as it burns without emitting soot or carbon dioxide. Nitrogen oxides NOx are the only potential pollutants from hydrogen combustion, and it is crucial to reduce NOx emissions from hydrogen combustion. Although the route leading to fuel NOx formation and destruction is still not completely understood, different investigators seem to agree on a simplified model:

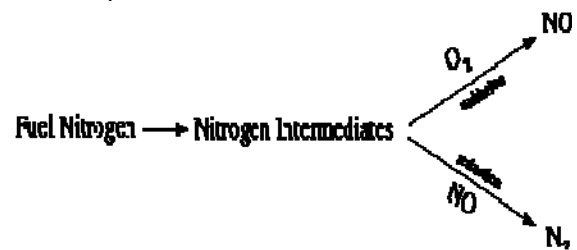


Fig 2. The route leading to fuel NOx formation

Recent investigations have shown that hydrogen cyanide appears to be the principal product if fuel nitrogen is present in aromatic or cyclic form. However, when fuel nitrogen is present in



the form of aliphatic amines, ammonia becomes the principal product of fuel nitrogen conversion. As NO constitutes the largest part of NO_x formed in combustion, its formation is calculated following Zeldovich mechanism in a manner similar to that followed by Ramos [13]. Since the initial step of this reaction mechanism involves very high activation energy, it is assumed that NO formation process is decoupled from the hydrocarbon combustion and occurs as a post combustion reaction process. The NO formation is governed by the following equations:



A steady state assumption made for the calculation of N atoms gives by:

$$\frac{d}{dt}(y_n) = 0 \quad (9)$$

The O atom is assumed to be in equilibrium with the O₂ molecule as:



where M is a third body. The rate of formation of NO is calculated as:

$$\frac{d}{dt}(y_{NO}) = k_1 y_{N_2} y_O - k_2 y_{NO} y_N + k_3 y_N y_{O_2} - k_4 y_{NO} y_O \quad (11)$$

The specific reaction rates K_1 – K_4 for the above reactions are taken from Ramos [13]. The species conservation equation for NO is solved with its rate of formation as the source term to

get NO concentration within the combustor as well as at the combustor exit. Pattern factor of a gas combustor is an index of uniformity of the temperature profile at the exit of the combustor. It is defined as:

$$Pattern\ factor = \left[\frac{T_{e\max} - T_{emean}}{T_{emean} - T_{in}} \right] \quad (12)$$

Where $T_{e\max}$ and T_{emean} are the maximum and bulk temperature of the gas at the combustor exit and T_{in} is the inlet air temperature to the combustor. The bulk mean temperature is determined as:

$$T_{emean} = \frac{\int_0^R 2\pi\rho T_e C_{pe} U_{ze} r dr}{\bar{C}_{pe} \int_0^R 2\pi\rho U_{ze} r dr} \quad (13)$$

The combustion efficiency for a given inflow of fuel is determined from the fuel vapour concentration at the combustor exit as follow:

$$\eta_c = 1 - \frac{2\pi \int_0^R \rho_e C_{fe} U_{ze} r dr}{\dot{m}_f} \quad (14)$$

Under the assumption of the adiabatic combustor wall, combustion efficiency depicts the quantity of energy that is converted from the energy stored in fuel to the thermal energy of the combustible mixture in the process of combustion.

3. Result and discussion

Many literatures have been focused to research about the combustion in micro-scale size, because numerical simulations could be



conducted for the same conditions as those in the experiments.

The combustion model at this study is validated by the measurement flame reported in Glassman (1996) and the numerical results in Jinsong Hua paper[1]. The comparison of flame temperature and mole fraction of species obtained from the model prediction and these results are listed in table 1. The results indicate that the numerical predictions are similar with the experimental data. Hence, these results can help to continue the researcher about pollution modeling.

Table1.Comparison of adiabatic flame temperature and mole fraction of species for H₂-air mixtures in experimental and numerical conditions

Temperature/ concentration	Experimental results (Glassman, 1996)	Numerical results (Jinsong Hua, 2005)	Numerical results (in present study)
Tb(k)	2382	2397	2410
H ₂ O	0.323	0.311	0.341
O ₂	0.005	0.009	0.0048
H ₂	0.015	0.02	0.01
N ₂	0.644	0.644	0.645

The flame temperature of various sized (a) 5mm (b) 0.4 mm (c) 0.2 mm (d) 0.05 mm under adiabatic wall condition display at "Fig .3" For comparing easily, the combustion temperatures along the central axis by the dimensionless axial distance for different diameters are shown at "Fig .4" These figures illustrate that the gas temperature is raised significantly due to the heat released from combustion. The highest temperature is obtained at the exit of combustion

chamber at a range of 2000–2800 K. Also the temperature of the combustion gas product decreases as the combustion chamber size decreases due to the incomplete combustion in smaller chambers. By using "Eq.(12)" pattern factor was achieved very nearly to zero for these various inlet diameters under adiabatic wall condition and this could be confirmed the uniformity of the temperature profile at the exit of the combustor.

Figure.5 illustrates that when the combustion chamber size propagates, the combustion efficiency increases. These results could be obtain by the "Fig.6" because when the chamber dimension is large enough, the gas mixture has enough residence time in the chamber, so that combustion will be completed before it flows out of the combustion chamber. Indeed, "Fig.6" by showing water production rate along the central axis of the chamber could be proven these results. Also, "Fig.6" shows that a narrow peak is formed for the large chambers due to the reaction confined to a narrow zone with the completed combustion and when combustion chamber size decreases the chemical reaction mechanism is kept same. Thus, the water production graphs represent that the decreasing of combustion chamber size does not have significant effect on the global reaction rate within the chamber.

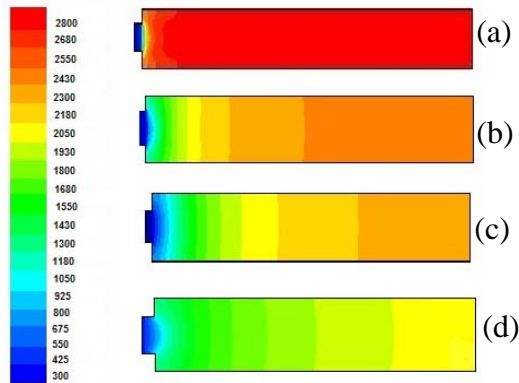


Fig.3 Temperature[k] contours on the cross section of combustion for different inlet diameters: (a) 5mm, (b) 0.4mm, (c) 0.2mm, and (d) 0.05mm, under adiabatic wall condition inlet velocity is 0.25m/s

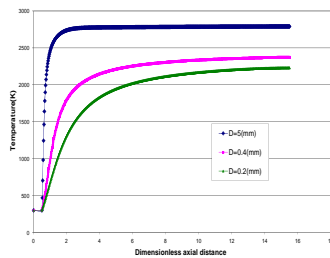


Fig.4 Gas temperature[k] plot on the central axis by different inlet diameters under adiabatic wall condition and inlet velocity is 0.25m/s

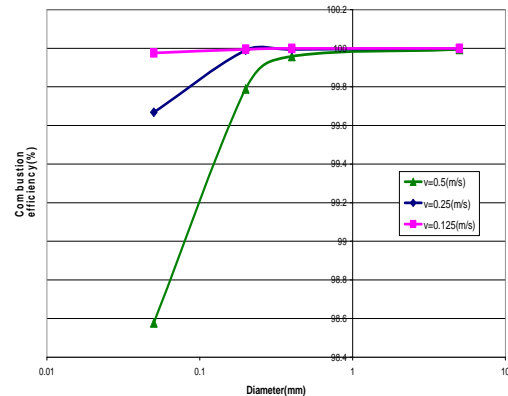


Fig.5 Combustion efficiency(%) for different inlet diameters under adiabatic wall condition and various inlet velocity

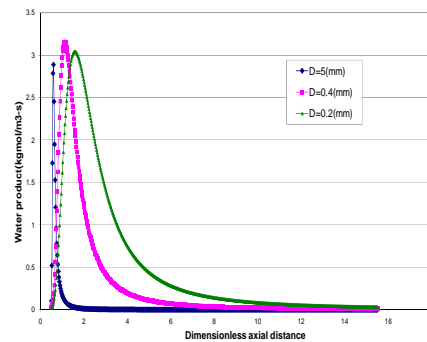


Fig.6 Water production rate [kgmol/m³-s] plot on the central axis by different inlet diameters under adiabatic wall condition and inlet velocity is 0.25m/s

These results indicate that, by increasing size of chamber the flame temperature is increased and the highest temperature is obtained at the exit of combustor. Also increasing the combustion chamber size and decreasing the inlet velocity propagates the combustion efficiency. The “Eq. (14)” could be confirmed these results. This is due to the fact that the gas mixture does not have enough residence time to finish the

and inlet



chemical reaction completely in the smaller chambers or high inlet velocity. Hence, to obtain a stable combustion in a micro-chamber, the chamber dimension should be larger.

“Fig.7” show the results of flame temperature contours of various sized combustion chambers with the inlet diameter of: (a) 5mm (b) 0.4 mm (c) 0.2 mm (d) 0.05 mm under adiabatic wall condition and NO_x emission. The results of “Fig.3” are similar to these results. Indeed, the highest temperature is obtained at the exit of combustion chamber at a range of 2000-2800K (as the same by “Fig.3 and 7”). Maximum values of NO_x emission profiles in different inlet diameter within the combustor at different operating conditions such as the velocities constant and the Reynolds number constant show at “Figs.8 and 9” respectively. These figures indicate that by increasing the diameter, decreasing the inlet velocity and the Reynolds number (due to decreasing velocity by raising inlet diameter for maintaining the Reynolds number at constant condition) the NO_x emission has great value, so that combustion will be completed before it flows out of the combustion chamber. But, maximum values of NO_x propagation at these profiles have a valley between small and large diameter (near 5 to 70 mm), it's may depend to the applicable condition of completed combustion. Indeed, periodical process of NO_x generation is recognized in two periods of combustion chamber diameter between 0.02 to 2 mm and between 2 to 500 mm which shows the rapid grow up NO_x will start after 10 percent of these periods. Also the

maximum values of NO_x emission is obtained at the exit of combustion chamber. Moreover, the result of numerical modeling of combustion pollutant was related that the rate of NO_x prompt for all diameters was been zero due to the fuel-air mixture wasn't hydrocarbon under fuel-rich condition.

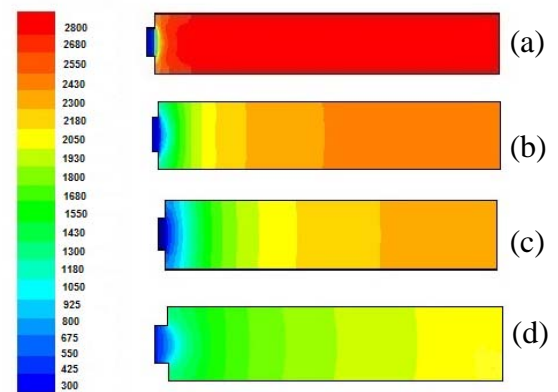


Fig.7 Temperature[k] contours of combustion chambers for different inlet diameters: (a) 5mm, (b) 0.4mm, (c) 0.2mm, and (d) 0.05mm, under adiabatic wall condition and inlet velocity is 0.25m/s

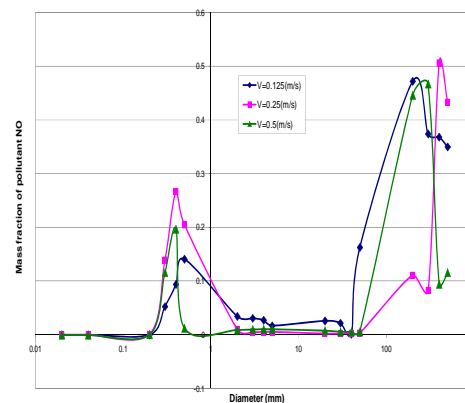


Fig.8 The maximum rate of mass fraction pollutant NO by different inlet diameters under inlet velocity constant and adiabatic wall conditions

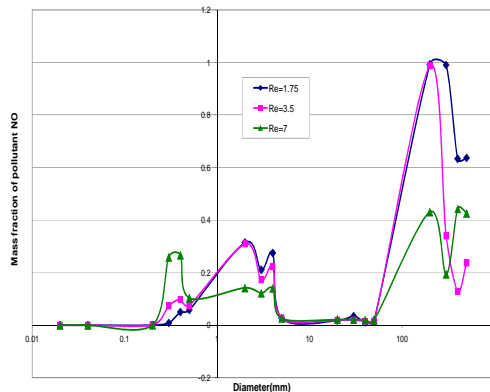


Fig.9 The maximum rate of mass fraction pollutant NO by different inlet diameters under inlet Reynolds number constant and adiabatic wall conditions

3. Conclusions

A numerical model has been used in this research to know the effect of changing the inlet diameter of chamber to temperature flame, combustion phenomena and the rate of mass fraction of pollutant of premixed hydrogen-air mixture under adiabatic wall condition. The results derived from this may study summarized as follows:

- 1- The flame temperature is increased by increasing size of chamber and the highest temperature is obtained at the exit of combustor.
- 2-Theoretically, high efficiency and stability of combustion obtains in large combustor size and the numerical results at this paper show it.
- 3- The mass fraction of pollutant NO_x didn't have any effect on temperature flame of H₂-air mixture combustion in micro scale chamber.
- 4- The mass fraction of pollutant is decreased by depleting size of chamber and the highest NO_x emission is obtained at the exit of combustor.

5- Hydrogen is a suitable fuel to reduce pollutant emissions, because of the zero emission of the prompt NO_x.

6- A micro combustor by great efficiency and lower pollutant emissions ought to have good diameter inlet such as between 5 to 70 mm.

4. References

4.1 Article in Journals

1. Jinsong, H., Meng, W. and Kurichi K. (2005). Numerical simulation of the combustion of hydrogen-air mixture in micro-scaled chambers. Part I: Fundamental study, Applied Chemical Engineering Science, vol.60, January 2008, pp. 3497 – 3506.
2. Epstein, A.H. and Senturia, S.D. (1997). Macro power from micro machinery, Applied Science. pp. 276-279.
3. Li a, J., Choua, S.K., Yang, W.M., Li, Z.W.(2009). A numerical study on premixed micro-combustion of CH₄-air mixture: Effects of combustor size, geometry and boundary conditions on flame temperature, Applied Chemical Engineering Journal, vol. 150, pp 213 –222.
4. Li, J. and Zhong, B. (2008). Experimental investigation on heat loss and combustion in methane/oxygen micro-tube combustor, Applied Thermal Engineering, vol.28, June 2007, pp 707–716.
5. Tien, J.H. and Stalker, R.J. (2002). Release of chemical energy by combustion in a supersonic mixing layer of hydrogen and air, Applied Combustion and Flame, vol.130, pp 329–348.



6. Norton, D.G. and Vlachos, D.G. (2003). Combustion characteristics and flame stability at the micro scale: a CFD study of premixed methane/air mixtures, *Applied Chemical Engineering Science*, vol.58, pp 4871–4882.
7. Norton, D.G. and Vlachos, D.G. (2004). A CFD study for propane/air micro flame stability, *Applied Combust Flame*, vol.138, pp 97–107.
8. Jinsong, H., Meng, W. and Kurichi, K. (2005). Numerical simulation of the combustion of hydrogen–air mixture in micro-scaled chambers. Part II: CFD analysis for a micro-combustor, *Applied Chemical Engineering Science*, vol.60, pp. 3507-3515.
9. Norton, D.G. and Vlachos, D.G. (2004). A CFD study of propane/air micro flame stability, *Applied Combust Flame*, vol.138, pp. 97-107.
10. Norton, D.G. and Vlachos, D.G. (2003). Combustion characteristics and flame stability at the micro scale: a CFD study of premixed methane/air mixtures, *Applied Chemical Engineering Science*, vol.58, pp. 4871-4882.
11. Kaisare, N.S. and Vlachos, D.G. (2007). Optimal reactor dimensions for homogeneous combustion in small channels, *Applied Catalysis Today*, vol. 120, January 2007, pp. 96–106.
12. J. Li, S.K. Chou, Z.W. Li and W.M. Yang (2008). A comparative study of H₂-air premixed flame in micro combustors with different physical and boundary conditions, *Applied Combustion. Theory and Modeling*, vol.12, April 2008, pp. 325–347.
13. Ramos, J.I. (1985). A numerical study of swirl stabilized combustors, *Applied Non-Equilibrium Thermodynamics*, vol. 10, June 1985, pp. 263-286.